

Spectropolarimetric Studies of Sunspot and its Fine-structure

A Thesis

submitted for the Award of Ph.D. degree of

MOHANLAL SUKHADIA UNIVERSITY

in the

Faculty of Science

By

Rahul Yadav



Under the supervision of

Dr. Shibu K. Mathew

Professor

Udaipur Solar Observatory

Physical Research Laboratory

Udaipur, India

DEPARTMENT OF PHYSICS

FACULTY OF SCIENCE

MOHANLAL SUKHADIA UNIVERSITY

UDAIPUR (RAJ)

Year of submission: 2017

DECLARATION

I, **Mr. Rahul Yadav**, S/o Mr. Ram Gopal Yadav, resident of C-2, USO staff quarters, Badi road, Udaipur-313001, hereby declare that the research work incorporated in the present thesis entitled, "**Spectropolarimetric studies of sunspot and its fine-structure**" is my own work and is original. This work (in part or in full) has not been submitted to any University for the award of a Degree or a Diploma.

I have properly acknowledged the material collected from secondary sources wherever required. I have run my entire thesis on the anti-plagiarism software namely, ".....".

I solely own the responsibility for the originality of the entire content.

Date:

Rahul Yadav
(Author)

CERTIFICATE

I feel great pleasure in certifying that the thesis entitled, "**Spectro-polarimetric Studies of Sunspot and its Fine-structure**" embodies a record of the results of investigations carried out by **Mr. Rahul Yadav** under my guidance. He has completed the following requirements as per Ph.D regulations of the University.

- (a) Course work as per the university rules.
- (b) Residential requirements of the university.
- (c) Regularly submitted six monthly progress reports.
- (d) Presented his work in the departmental committee.
- (e) Published minimum of one research papers in a referred research journal.

I recommend the submission of thesis.

Date:

Dr. Shibu K. Mathew
(Thesis Supervisor)
Udaipur Solar Observatory,
Physical Research Laboratory,
Udaipur - 313 001.

Countersigned by

Head of the Department

To

My Family

Acknowledgements

It is my great pleasure to express my gratitude to my supervisor Prof. Shibu K. Mathew for his invaluable guidance, encouragement and support throughout my Ph.D. tenure. I am grateful to him for accepting me as his student and giving me this wonderful opportunity to work at Udaipur Solar Observatory. His dedication towards work always motivates me to do good work.

I am thankful to the Director and the Dean of PRL for providing the necessary facilities required during this work. I would like to thank the academic committee members of PRL for reviewing my work regularly. I express my sincere gratitude to the faculty members of USO, Prof. P. Venkatakrishnan (former Head of USO), Prof. Ashok Ambastha, Dr. Ramitendra Bhattacharyya, Dr. Bhuvan Joshi, and Dr. Ankala Raja Bayanna for their support and encouragement at various stages of my thesis. I would like to thank my thesis experts Prof. Nandita Srivastava and Dr. Brajesh Kumar for reviewing my thesis. Thanks are due to all the other staff members of USO, Mr. Raju Koshy, Ms. Ramya Bireddy, Mr. Rakesh Jaroli, Mr. Naresh Jain, Mr. Mukesh M. Saradava, Mr. Harsh Chopra, Mr. Sudharshan Jain and all the past and present trainees for their help and support at various stages of my thesis. I would like to extend my thanks to Mr. Jigar Raval and all the staff members of PRL computer center for their support.

It is my pleasure to acknowledge the science team of SOHO/MDI, SDO/HMI and Hinode for providing the excellent quality data. Hinode is a Japanese mission developed and launched by ISAS/JAXA, collaborating with NAOJ as a domestic partner, NASA and STFC (UK) as international partners. Scientific operation of the Hinode mission is conducted by the Hinode science team organized at ISAS/JAXA. This team mainly consists of scientists from institutes in the partner countries. Support for the post-launch operation is provided by JAXA and NAOJ (Japan), STFC (U.K.), NASA, ESA, and NSC (Norway).

I would like to express my sincere gratitude to Dr. Juan Manuel Borrero for providing us with the VFISV-TEST code. Without his support and help the development of SPIN code would have been very difficult. I am eternally grateful

to him. I further extend my thanks to Prof. J. C. del Toro Iniesta for fruitful discussions on inversion codes in Granada. I also acknowledge his wonderful book ‘Introduction to Spectropolarimetry’ which helped me in understanding the inversion techniques. I express my sincere gratitude to Dr. Rohan Eugen Louis for his guidance and scientific discussions which deepened my knowledge in the area of my research.

It is my pleasure to express my sincere gratitude to all my teachers for their motivation and encouragement.

I would like to thank my seniors Drs. Suruchi Goel, Vema Reddy Panditi, Dinesh Kumar, Upendra Kushwaha, Wageesh Mishra, Sanjay Kumar, Alok R. Tiwary, Gaurava Jaiswal, Arun K. Pandey, Yashpal Singh, Gaurav Kumar, Gulabhbhai Bambaniya, Abhay Swain, Tammooy Mandal, Tanmoy Chattopadhyay, Monojit Ghosh, Guruprasad Kadam and Girish Kumar for helping me at various stages of my thesis work. I would like to also extend my thanks to my juniors Hemant, Ranadeep, Susree, and Prabeer for enjoyable days at USO.

I thank all my batch-mates: Newton, Chandana, Jinia, Lalit, Ashim, Pankaj, Deepak, Dipti, Bivin, Venkatesh, Sukkanaya, Prashant, Apurv, Rajat, Samiran, Sanjay, Mangalanand, Vikas, and Anand for making my stay at PRL comfortable and enjoyable.

I extend my thanks to Drs Sowmya K., Supriya H. D., Sindhuja G., Avijeet Prasad, Sajal Kumar Dhara, and Mr. Mohanakrishna for their support and cooperation.

I would like to thank Ghyaneneder Singh Lakra and Swapnil Mahajan for their continuous support and motivation throughout my Ph.D. tenure.

I indebted to all my friends who have contributed directly or indirectly in this thesis work.

Last but not the least, I express my sincere gratitude to my family for their encouragement, love and affection. This thesis would not have been possible without the blessings and support of my parents. I express my sincere gratitude to my ‘supercool-amma’ for making my childhood special.

ABSTRACT

Solar activity is governed by the magnetic fields, which are ubiquitously distributed on small or large spatial scales on the Sun. The interaction of the magnetic fields with vigorous convection on the solar surface manifests itself in the different form of structures. Among these, the sunspots (~ 30000 km) and the pores (~ 4000 km) are the most prominent manifestations of the magnetic fields which are observed frequently on the photosphere depending on solar activity. Predominantly, the sunspots harbor strong magnetic fields (~ 3000 G), which are responsible for solar activities such as flares and coronal mass ejections. These activities cause fluctuations in the solar irradiance which directly influences the solar atmosphere and ultimately the space weather and the Earth. A better understanding of solar activities demands a careful investigation of sunspot's formation and stability, which is yet to be fully understood. The high-resolution observations of sunspots have revealed the presence of fine-structures of sunspots such as umbral dots, penumbral filaments and grains, which can play an important role in understanding the physical nature of sunspots. The study of sunspot fine-structures, using high-resolution imaging and spectro-polarimetric observations, can provide us insights on the evolution and stability of the sunspots, and can give crucial inputs to the realistic sunspot models.

The magnetic and thermodynamical properties of the solar atmosphere are generally inferred from the interpretation of observed Stokes profiles using inversion techniques. The inferred solar atmosphere can be utilized in understanding the physical mechanism of the solar features. This thesis aims at undertaking studies in this direction and comprises of two parts. The first part includes the development of a Milne-Eddington based Stokes profile inversion (SPIN) code for the polarized radiative transfer equation, which will be dedicated to invert the photospheric spectro-polarimetric data obtained from the Multi-Application Solar Telescope (MAST). The SPIN code can be employed to interpret the Stokes profiles in order to infer the magnetic and kinematic properties of the solar photosphere. The second part of the thesis is focused on the understanding of

the physical properties of umbral dots, which are the transient dot-like bright features observed in the dark umbra of a sunspot. The high-resolution observations obtained by *Hinode*, a Japanese space-based observatory, are utilized to investigate the physical properties of umbral dots and their relation with the macroscopic-properties of sunspots such as, size, epoch, decay rate and filling factor.

The thesis is organized in the following way. In Chapters 1 and 2, we present some of the basic concepts and discuss the solar features which are necessary for understanding the contents of the thesis. Chapter 3 presents the details of SPIN code developed specifically to invert the MAST's spectro-polarimetric data. The SPIN code has adopted the Milne-Eddington approximations to solve the polarized radiative transfer equation (*i.e.*, synthesis of Stokes profiles). A modified Levenberg-Marquardt algorithm has been employed to minimize the differences between the observed and the synthetic Stokes profiles. We also present the details of the tests performed to validate the SPIN code by comparing the results from the other widely used inversion codes namely, MERLIN, VFISV and SIR. In this regard, we have used the spectro-polarimetric data obtained from the *Hinode* spacecraft. The retrieved physical parameters obtained after the inversion of an active region using SPIN and other inversion codes exhibit similar results. Physical parameters of an active regions such as magnetic field strength, line-of-sight (LOS) velocity, inclination and azimuthal angle can be readily inferred with SPIN. This code is capable to invert any single photospheric Zeeman triplet spectral line.

Chapter 4 gives a brief overview of the spectro-polarimeter (SP) integrated with the MAST. The data acquisition and reduction of the spectro-polarimetric data recorded by the MAST/SP is discussed in detail. We also present the line-of-sight (LOS) magnetic field (B_{los}) retrieved after the inversions of MAST/SP data using SPIN code and its comparison with the B_{los} obtained from the space-based telescope (HMI/SDO). The comparison reveals that both the instruments (MAST/SP and HMI/SDO) exhibit similar B_{los} values across an active regions, considering the fact that MAST observations, unlike HMI/SDO, are limited by

seeing. In addition to this, we carried out the inversions of an active region, recorded with MAST/SP, using 6, 8, 11 and 20 wavelength samples across Fe I 6173 Å spectral line to see the effects of number of wavelength samples on inverted parameters. We found that for MAST/SP, the inversion with different wavelength samples can exhibit similar results. We also noticed that increase in the wavelength samples above 8 does not produce significant improvements, whereas a decrease produces worse results. The mean standard deviation of B_{los} maps (relative to 20 wavelength samples) obtained in umbral regions with 11, 8 and 6 spectral positions are 53 G, 241 G, and 363 G, respectively.

In Chapter 5, we present the details of the analysis carried out using high-resolution *Hinode*/SOT G-band time-series of seven active regions observed close to disk center. In these studies, the umbral dots (UDs) are identified and tracked using an automated identification and tracking algorithm in all seven sunspots. We have also discussed the use of MDI continuum images to estimate the decay rate of selected sunspots. The statistical analysis of UDs exhibit the averaged maximum intensity and effective diameter of $0.26 I_{QS}$ and 270 km, respectively. Further, we found that the lifetime, horizontal speed, trajectory length, and displacement length (birth-death distance) of UDs are 9.85 minutes, 0.5 km s^{-1} , 284 km, and 155 km, respectively. We also find a positive correlation between intensity – diameter, intensity – lifetime, and diameter – lifetime of UDs. The results from our studies exhibit that the properties of UDs do not show any significant relation with the decay rate and filling factor of sunspots.

In Chapter 6, we present the investigation of the relation between the physical properties of UDs and the macro-properties of a sunspot. For this purpose, we analyzed high-resolution G-band images of 42 sunspots observed by *Hinode*/SOT, located close to disk center. All the images are corrected for instrumental stray-light and restored with the modeled PSF. An automated Multi-Level Tracking algorithm employed to identify the UDs located in selected G-band images is discussed. Furthermore, a method to estimate the sunspot evolving phase and epoch for the selected sunspots using HMI/SDO, limb-darkening corrected, full disk continuum images is also presented. The number of UDs identified in dif-

ferent umbrae exhibit a linear relation with the umbral size. However, we do not find any significant relationship between the mean intensity and effective diameter of umbral dots with the sunspot area, epoch, and decay rate. The observed filling factor ranges from 3% to 7% and increases with the mean umbral intensity. Moreover, the filling factor shows a decreasing trend with the umbral size. We also found that the observed intensities of UDs is correlated with the mean umbral intensity.

Chapter 7 provides the summary and conclusions of the thesis work. In this chapter, we also present a brief description of the future work.

Keywords : Photosphere, Sunspot, Magnetic fields, Umbral dots

LIST OF PUBLICATIONS

1. “*Imaging Spectropolarimeter for Multi-Application Solar Telescope at Udaipur Solar Observatory: Characterization of Polarimeter and Preliminary Observations*”.
Alok Ranjan Tiwary, Shibu K. Mathew, A. Raja Bayanna, P. Venkatakrishnan and **Rahul Yadav**, *Solar Phys.* (2017) 292(4), 49.
DOI. <http://dx.doi.org/10.1007/s11207-017-1076-5>.
2. “*SPIN: An Inversion Code for the Photospheric Spectral Line*”
Rahul Yadav, Shibu K. Mathew and Alok Ranjan Tiwary, *Solar Phys.* (2017) 292:105. <https://doi.org/10.1007/s11207-017-1131-2>
3. “*Investigating the Relation between Sunspots and Umbral Dots*”
Rahul Yadav, Rohan E. Louis and Shibu K. Mathew, *Astrophys. J.* (2017), *under review*
4. “*Physical Properties of Umbral Dots observed in Sunspots: A Hinode observation*”
Rahul Yadav and Shibu K. Mathew, *Solar Phys.* (2017), *under review*

Contents

Acknowledgements	i
Abstract	iii
List of Publications	vii
List of Figures	xii
List of Tables	xvii
1 Introduction	1
1.1 The Sun	1
1.2 The Structure of the Sun	3
1.3 Sunspots	6
1.4 The fine-structures of sunspots	10
1.4.1 Umbral dots	11
1.4.2 Light bridges	14
1.4.3 Penumbral filaments and grains	15
1.5 Magnetic field measurements in photosphere and chromosphere .	16
1.6 The observational data and instruments	19
1.6.1 <i>Hinode</i> /SOT	19
1.6.2 The Solar Dynamics Observatory (SDO)	22
1.6.2.1 The Helioseismic and Magnetic Imager (HMI) .	24
1.6.3 The Multi-Application Solar Telescope	24
1.7 Motivation and organization of the thesis	29

2 Spectro-polarimetry	32
2.1 Introduction	32
2.2 Polarization states of light	33
2.2.1 Stokes parameters	34
2.2.2 The measurement of Stokes parameters	36
2.3 Zeeman effect	39
2.4 Polarized Radiation Transfer	43
2.5 Solution of the RTE	47
2.5.1 Milne-Eddington approximation	50
2.6 Summary	53
3 SPIN: An Inversion Code for the Photospheric Spectral Line	54
3.1 Introduction	54
3.2 Introduction to inversion codes	55
3.3 Motivation for a new inversion code: SPIN	57
3.4 Milne-Eddington inversion procedure	59
3.5 Response functions	63
3.6 Synthetic module tests	68
3.7 Merit function, convergence and limits	70
3.7.1 Initial guess model	72
3.7.2 Limits on parameters	75
3.8 Inversion module tests	76
3.8.1 Fitting of known Stokes profiles	76
3.8.2 Test with real observations: <i>Hinode</i> /SP Data	78
3.9 Comparison with other inversion codes	85
3.10 Reliability of M-E inversion	89
3.11 Summary	91
4 Polarimetry with MAST	92
4.1 Introduction	92
4.2 Configuration of MAST	93
4.3 Imaging Spectro-polarimeter	95

4.3.1	Instrumental smearing effect	98
4.4	Multi-Slit Spectro-Polarimeter	100
4.5	Inversion of MAST/SP data	102
4.5.1	Dark current and flat-field correction	102
4.5.2	Observation of NOAA AR 12648	103
4.5.2.1	Comparison of LOS magnetic field	104
4.5.3	Observations of NOAA AR 12653 with MAST/MSSP . . .	106
4.5.3.1	Comparison of LOS magnetic field	108
4.5.4	Inversion with different number of wavelength samples . .	109
4.6	Summary	111
5	Physical properties of Umbral Dots	113
5.1	Introduction	113
5.2	Observations and data reduction	114
5.2.1	Sunspot area calculation	117
5.3	Identification of Umbral dots and tracking	119
5.3.1	Identification of UD	119
5.3.2	Tracking of UDs	121
5.4	Results and Discussion	122
5.4.1	Physical properties of UDs	122
5.4.1.1	Size	122
5.4.1.2	Intensity	125
5.4.1.3	Lifetime	126
5.4.1.4	Horizontal velocity	126
5.4.1.5	Trajectory	127
5.4.2	Correlation between various UDs properties	129
5.5	Summary and conclusions	131
6	Investigating the Relation between Sunspot and Umbral Dots	134
6.1	Introduction	134
6.2	Observations and data analysis	135
6.2.1	Instrumental stray-light correction	136

6.2.2	Sunspot epoch, decay and growth rate	140
6.3	Identification of UDs	142
6.4	Results	143
6.4.1	Umbral size, intensity and number of UDs	144
6.4.2	UD intensity and size	146
6.4.3	UD parameters versus the area change and epoch of sunspots	149
6.5	Discussion	149
6.6	Summary	153
7	Summary and Future Work	154
7.1	Future work	157
Appendix A		160
A.1	Derivatives of χ^2 and response functions	160
Appendix B		163
B.1	Start and run SPIN	163
B.2	The SPIN input file	164
B.3	Output files	166
Appendix C		168
C.1	Inversion of <i>Hinode</i> /SP data using SPIN	168
Bibliography		171
Publications attached with the thesis		179

List of Figures

1.1	A diagram showing different internal and outer parts of the Sun	3
1.2	Sketch of the internal structure of the Sun and solar atmosphere	4
1.3	Plasma- β as a function of height is shown for two assumed field strengths, 100 G and 2500 G	5
1.4	The solar photosphere observed in G-band with the Solar Optical Telescope on-board the <i>Hinode</i> Satellite	6
1.5	Sunspot activity over the last four hundred years	8
1.6	A simple sketch of emergence of flux tubes forming a pair of sunspots	9
1.7	Sketch of the monolithic and cluster models	10
1.8	Cartoon representation of an UD in the cluster model	12
1.9	Simulated UDs in the monolithic models	13
1.10	Block diagram of the inversion procedure under NLTE and LTE assumptions	18
1.11	Optical schematic of the OTA and FPP instruments	20
1.12	A sunspot observed by SOT/SP on November 20, 2013 (05:00 to 05:24 UT)	21
1.13	MAST's telescope floor within the collapsible dome.	26
1.14	Simultaneous images in H-alpha and G-band observed from MAST	28
2.1	Polarized states of light for a monochromatic wave	35
2.2	<i>Right panel:</i> a linear retarder with fast axis along the X-coordinate	37
2.3	Pictorial representation of the Stokes profiles	38
2.4	Allowed transition ($\Delta J = 0, \pm 1$ and $\Delta M_J = 0, \pm 1$) between the Zeeman split levels	40

2.5	The polarization properties of the radiation emitted by different Zeeman components	41
2.6	The magnetic field vector orientation in the observer's reference frame	44
2.7	Propagation matrix elements of a Zeeman triplet (Fe I 6173.34 Å) .	46
2.8	The synthetic Stokes profiles (I , Q , U , V) generated from the RTE solution under M-E approximation	50
2.9	All four Stokes profiles are synthesized for Fe I 6173.34 Å spectral line	52
3.1	A block diagram for the iterative fitting process of M-E inversion code.	61
3.2	Comparison of analytical and numerical RFs with respect to B . .	64
3.3	Comparison of analytical and numerical RFs with respect to θ . .	64
3.4	Comparison of analytical and numerical RFs with respect to φ . .	65
3.5	Comparison of analytical and numerical RFs with respect to V_{los} .	66
3.6	Analytical M-E RFs of Stokes profiles with respect to B , θ , and φ	67
3.7	Analytical M-E RFs of Stokes profiles with respect to V_{los} , λ_D , and a	68
3.8	Analytical M-E RFs of Stokes profiles with respect to η_0 , S_0 , and S_1	69
3.9	Comparison of all four Stokes profiles generated form the SPIN and the VFISV	71
3.10	Guess value of V_{los} is determined (using $\delta\lambda$) by fitting Stokes I with a Gaussian function	73
3.11	A comparison between initialized and inverted values for the magnetic field strength and inclination angle	74
3.12	Magnetic field strength map, obtained after the inversion of Hinode/SP data for NOAA AR 11330	76
3.13	The synthetic profiles and best fitted Stokes profiles	77
3.14	The scatter plot show the residual values for different M parameters (B , θ , ϕ , and V_{los})	79

3.15	The scatter plots represent the residual values obtained after the subtraction of the known and retrieved parameters	80
3.16	The normalized continuum intensity map of AR 11330 observed from <i>Hinode</i> /SP and observed Stokes <i>I</i> profile for a quiet-sun pixel	80
3.17	Observed (dots) and best-fitted (red line) Stokes profiles in AR 11330 recorded by <i>Hinode</i> /SP	81
3.18	Inverted parameters retrieved after inverting the <i>Hinode</i> /SP data for active region AR 11130	82
3.19	The inverted map of azimuthal angle before and after 180° ambiguity correction	83
3.20	The errors retrieved by SPIN in physical parameters after inverting active region AR 11330	84
3.21	The magnetic field map obtained after the inversion of AR 11330 using SIR and SPIN	86
3.22	The residual values obtained after subtracting the physical parameters inferred from the SIR and the SPIN inversion codes	86
3.23	The retrieved physical parameter maps obtained after the inversion of NOAA AR 11330, using three M-E based inversion codes .	87
3.24	One to one relation between the physical parameters obtained from three different inversion codes	88
3.25	LTE source function for various atmospheric models as a function of optical depth (τ_c)	90
4.1	The optical layout of MAST telescope and a snapshot showing the telescope structure mounted on top of the observing building . . .	93
4.2	A block diagram of imaging spectro-polarimeter for MAST	95
4.3	BASS2000 solar survey spectral atlas around the Fe I 6173 Å spectral region and illustration of tuning of a narrow-band filter	96
4.4	Maps of Stokes <i>I</i> , <i>Q</i> , <i>U</i> and <i>V</i> for Fe I 6173.34 Å , observed on 1st April, 2017 in AR 12645 using MAST’s imaging spectro-polarimeter.	97
4.5	Synthetic and convolved Stokes profiles (<i>I</i> , <i>Q</i> , <i>U</i> , and <i>V</i>)	99

4.6	The Optical layout of MSSP.	100
4.7	The Stokes I , Q , U and V spectra of the Fe I 6301.5 and 6302.5 Å spectral lines observed from MAST/MSSP	101
4.8	The continuum intensity maps of AR 12645 before (a) and after (b) dark current and flat-field corrections.	103
4.9	The continuum intensity map and Stokes V map of AR 12648 observed by MAST's imaging spectro-polarimeter.	104
4.10	The observed and best fitted Stokes (I and V) profiles obtained after the inversion of AR 12648 from SPIN.	105
4.11	The retrieved B_{los} obtained from MAST/SP and HMI/SDO . . .	105
4.12	Continuum map of NOAA AR 12653 observed by HMI/SDO (<i>left panel</i>) and MSSP/MAST (<i>right panel</i>).	107
4.13	The retrieved LOS magnetic field maps of NOAA AR 12653 from HMI/SDO (<i>left panel</i>) and MAST/MSSP data (<i>middle panel</i>). . .	108
4.14	The Continuum intensity map and LOS magnetic field strength .	110
4.15	The B_{los} maps obtained after the inversion of NOAA AR 12651 using SPIN code.	110
5.1	MDI full disk master flat-field image for January 2007 and position of selected sunspots	116
5.2	The decay rate of a sunspot is shown.	117
5.3	Demonstration of image segmentation method to identify the umbral dots.	120
5.4	Intensity profiles of a tracked UD is shown	122
5.5	The physical properties of observed in selected active regions . .	123
5.6	The histogram of various UD properties observed in seven different sunspots.	124
5.7	The scatter plots of all UDs observed in seven active regions . .	128
5.8	The relation between UDs physical properties and decay rates of seven sunspots	130

5.9	The relation between UDs physical properties and filling factor for selected sunspots	131
6.1	The filled black circles depict the locations of the selected sunspots during <i>Hinode</i> observations on the artificial solar disk	136
6.2	Sunspot in NOAA AR 12227 shown before (a) and after (b) stray-light correction	139
6.3	The decay rate of a sunspot is shown. The filled circles represents area value of a sunspot (AR NOAA 11974)	141
6.4	The decay rate of a sunspot is shown. The filled circles represents area value of a sunspot (AR NOAA 11974)	142
6.5	SC image of a sunspot observed in NOAA AR 11921, the red color closed contour defines the penumbra–umbra boundary	143
6.6	From top to bottom - variation of the mean umbral umbral intensity, number of UDs, and filling factor as a function of the umbral diameter for the stray-light corrected images.	144
6.7	Scatter plot between filling factor and the mean umbral intensity .	146
6.8	Scatter plot between the maximum UD intensity and umbra diameter	147
6.9	Scatter plots showing the relation of maximum intensity of UDs with the mean umbral intensity observed in 42 different umbrae .	148
6.10	Scatter plots depict the relation of maximum UD intensity with respect to the sunspot area change and epoch.	148
B.1	IDL widget showing the synthetic module and inversion module of SPIN	167
C.1	Inverted parameters retrieved after the inversion of AR 11899 (observed by <i>Hinode</i> /SP) using SPIN code	169
C.2	Same as Figure C.1 but for AR 11944.	170

List of Tables

1.1	Physical properties of the Sun.	2
1.2	HMI specifications	23
1.3	HMI observables	23
1.4	Specifications of MAST	26
1.5	Spectro-polarimeter for MAST	27
1.6	MAST's back-end instruments	27
2.1	Analytical expressions for the strength of the Zeeman components	42
3.1	Examples of available inversion codes.	57
3.2	Atomic parameters for the spectral lines used in the inversion . .	70
3.3	Limits on the model parameters.	74
3.4	A comparison of real and retrieved values after the inversion of known Stokes profiles shown in Figure 3.13.	78
5.1	Parameters of selected sunspots observed in G-band channel. . .	115
5.2	The decay rate of sunspots observed in different active regions. The parenthesis represents the standard deviation in the decay rate.	115
5.3	Average values of UD properties observed in different active regions	127
5.4	Physical properties of all combined umbral dots	129
5.5	Linear correlation coefficient (CC) between various physical properties of umbral dots	129
6.1	Details of the ARs analysed in the study	137

6.2	The physical properties of UDs observed in the stray-light corrected images (see Table 6.1)	138
6.3	Fit parameters for the power law ($y = A \times x^B$; Figures 6.6(a – b)) and linear ($y = A + Bx$; Figures 6.6(c – f), 6.7 – 6.9) functions	150
B.1	Spin input file	165

Appendices

Appendix A

A.1 Derivatives of χ^2 and response functions

In Chapter 3 (Equation 3.4.3), we have defined the merit function (χ^2). The derivative of χ^2 with respect to a parameter (say, x_p) is used to evaluate the Hessian matrix which determines the changes in the parameters for the next iteration. More details about the derivatives can be found in (del Toro Iniesta 2003; Borrero et al. 2011) and (Orozco Suárez and Del Toro Iniesta 2007).

As defined in Chapter 3, response functions (R_p) are the partial derivative of the Stokes vector, $\mathbf{I} = [I, Q, U, V]$, with respect to the model parameters (x_p),

$$R_p(\lambda_i) = \frac{\partial \mathbf{I}^{syn}(\lambda_i, \mathbf{M})}{\partial x_p} \quad (\text{A.1.1})$$

The first and second order of χ^2 in the form of response functions can be expressed as,

$$\frac{\partial \chi^2}{\partial x_p} = \frac{-2}{4N - F} \sum_{i=1}^N \sum_{j=1}^4 [\mathbf{I}_j^{obs}(\lambda_i) - \mathbf{I}_j^{syn}(\lambda_i, \mathbf{M})] \frac{\omega_j^2}{\sigma_j^2} \times R_p(\lambda_i), \quad (\text{A.1.2})$$

$$\frac{\partial \chi^2}{\partial x_p \partial x_k} = \frac{-2}{4N - F} \sum_{i=1}^N \sum_{j=1}^4 \frac{\omega_j^2}{\sigma_j^2} \left\{ R_p(\lambda_i) R_k(\lambda_i) + [\mathbf{I}_j^{obs}(\lambda_i) - \mathbf{I}_j^{syn}(\lambda_i, \mathbf{M})] \frac{R_p(\lambda_i)}{\partial x_k} \right\}, \quad (\text{A.1.3})$$

Neglecting the derivative of the response function in Equation (A.1.3), the equation can be expressed as,

$$\frac{\partial \chi^2}{\partial x_p \partial x_k} \simeq \frac{-2}{4N - F} \sum_{i=1}^N \sum_{j=1}^4 \frac{\omega_j^2}{\sigma_j^2} [R_p(\lambda_i) R_k(\lambda_i)]. \quad (\text{A.1.4})$$

Thus, from above Equation (A.1.4) it can be seen that the Hessian matrix elements can be written in terms of the response functions. In M-E atmosphere, they can be calculated analytically which significantly enhance the computing speed. It can be seen that the derivative of Stokes parameters with respect to the S_0 and S_1 is straightforward to evaluate. The Stokes parameters shown in Equation (2.5.14) are functions of elements of propagation matrix. Thus, the derivative of the propagation matrix elements with respect to the model parameters ($[\eta_0, \Delta\lambda_D, a, S_0, S_1, B, \theta, \phi, V_{los}]$) are required. The derivative of the elements with respect to η_0 can be expressed as,

$$\begin{aligned} \frac{\partial \eta_I}{\partial \eta_0} &= (1 - \eta_I)/\eta_0, \\ \frac{\partial \eta_Q}{\partial \eta_0} &= \eta_Q/\eta_0, \\ \frac{\partial \eta_U}{\partial \eta_0} &= \eta_U/\eta_0, \\ \frac{\partial \eta_V}{\partial \eta_0} &= \eta_V/\eta_0. \end{aligned} \quad (\text{A.1.5})$$

The derivatives with respect to θ and φ ,

$$\begin{aligned} \frac{\partial \eta_I}{\partial \theta} &= \frac{\eta_0}{2} \left\{ \phi_p - \frac{(\phi_b + \phi_r)}{2} \right\} \sin 2\theta, \\ \frac{\partial \eta_Q}{\partial \theta} &= \frac{\eta_0}{2} \left\{ \phi_p - \frac{(\phi_b + \phi_r)}{2} \right\} \sin 2\theta \cos 2\varphi, \\ \frac{\partial \eta_U}{\partial \theta} &= \frac{\eta_0}{2} \left\{ \phi_p - \frac{(\phi_b + \phi_r)}{2} \right\} \sin 2\theta \sin 2\varphi, \\ \frac{\partial \eta_V}{\partial \theta} &= -\eta_V \tan \theta, \\ \frac{\partial \eta_Q}{\partial \theta} &= \frac{\eta_0}{2} \left\{ \psi_p - \frac{(\psi_b + \psi_r)}{2} \right\} \sin 2\theta \cos 2\varphi, \\ \frac{\partial \eta_U}{\partial \theta} &= \frac{\eta_0}{2} \left\{ \psi_p - \frac{(\psi_b + \psi_r)}{2} \right\} \sin 2\theta \sin 2\varphi, \\ \frac{\partial \eta_V}{\partial \theta} &= -\eta_V \tan \theta, \end{aligned} \quad (\text{A.1.6})$$

$$\begin{aligned}
\frac{\partial \eta_I}{\partial \varphi} &= \frac{\partial \eta_V}{\partial \varphi} = \frac{\partial \rho_V}{\partial \varphi} = 0, \\
\frac{\partial \eta_Q}{\partial \varphi} &= -2\eta_Q \tan 2\varphi, \\
\frac{\partial \eta_U}{\partial \varphi} &= 2\eta_U \cot 2\varphi, \\
\frac{\partial \rho_Q}{\partial \varphi} &= -2\rho_Q \tan 2\varphi, \\
\frac{\partial \rho_U}{\partial \varphi} &= 2\rho_U \cot 2\varphi.
\end{aligned} \tag{A.1.7}$$

To evaluate the derivatives with respect to other parameters (a , $\Delta\lambda_D$, V_{los} and B), we need to evaluate the derivatives of the Voigt and Faraday functions (Equation 2.4.4 and 2.4.5), which can be expressed by applying chain rule as,

$$\begin{aligned}
\frac{\partial H(v, a)}{\partial V_{los}} &= \frac{\partial H(v, a)}{\partial v} \frac{\partial v}{\partial V_{los}}, \\
\frac{\partial H(v, a)}{\partial \Delta\lambda_D} &= \frac{\partial H(v, a)}{\partial v} \frac{\partial v}{\partial \Delta\lambda_D}, \\
\frac{\partial H(v, a)}{\partial B} &= \frac{\partial H(v, a)}{\partial v} \frac{\partial v}{\partial B}.
\end{aligned} \tag{A.1.8}$$

The expressions for $F(v, a)$ are same as Equation A.1.8. The derivatives of the Voigt and Faraday-Voigt function can be expressed as,

$$\begin{aligned}
\frac{\partial H(v, a)}{\partial v} &= 2aF(v, a) - 2vH(v, a), \\
\frac{\partial F(v, a)}{\partial v} &= \sqrt{4/\pi} - 2aH(v, a) - 2vF(v, a), \\
\frac{\partial H(v, a)}{\partial a} &= -\frac{\partial F(v, a)}{\partial v}, \\
\frac{\partial F(v, a)}{\partial a} &= \frac{\partial H(v, a)}{\partial v}.
\end{aligned} \tag{A.1.9}$$

Appendix B

B.1 Start and run SPIN

In this appendix, we provide a brief information about the operation of SPIN. All the subroutines of SPIN have been written in IDL programming language and it also uses some routines available in SSW* packages. The SPIN folder contains the following routines:

1. **spin_input.txt**: This is the spin input file which contain all required initial inputs. More details can be found in Section B.2.
2. **spininv.pro**: This is the main routine which reads *spin_input.txt* file and calls other subroutines.
3. **syn_prof.pro**: This routine solves all four Stokes profiles analytically.
4. **respfun.pro** : The response functions of all Stokes profiles with respect to a particular model parameter are evaluated by this routine.
5. **lminv.pro**: This routine minimizes the difference between the observed and synthetic Stokes profiles.
6. **merit.pro**: The evaluation of Hessian matrix and merit function (χ^2).
7. **svdcal.pro**: To perform the singular value decomposition of Hessian matrix.
8. **fvoigt.pro**: Evaluation of Faraday and Voigt-Faraday function.

*More details can be found at: <http://www.lmsal.com/solarsoft/>

9. **limits.pro**: This routine impose limits on the model parameters.
10. **macvel.pro**: Evaluates the macro-turbulence velocity.
11. **readinput.pro**: To read the input file.
12. **guess_mod.pro**: It estimates the guess model parameters based on weak field approximation.
13. **calpol.pro**: Evaluates the polarization level of pixels.
14. **plotstk.pro**: Used to plot the fitted and observed Stokes profiles.
15. **combine.pro**: It combines all inverted maps.
16. **view_profiles.pro**: To view interactively the observed and synthetic Stokes profiles for a pixel.

B.2 The SPIN input file

The SPIN is performed and controlled by the *spin_input.txt* file. The input parameters required to run SPIN are given in Table B.1. Presently, there are 24 lines in input files. The first column refers to the input variable name, the colon mark (:) in second column separated the input variable name and their corresponding inputs (column three). We describe briefly the variables used in the input file:

- **cycle-number**: This parameter indicates the number of inversion cycle to be performed for a single pixel.
- **obs-profiles (sav-file)**: It refers the name of standard IDL savefile where the observed Stokes profiles are stored in a 3D array. As an example, the format for the Stokes I is $[xpixels, ypixels, \lambda]$.
- **weight-Stokes[I, Q, U, V]**: The weights for Stokes I , Q , U and V used in the χ^2 are given in line 3, 4, 5, 6, respectively.

- **wavelength:** The inversion carried out for this wavelength. For Fe I 6173.334 Å, and Fe I 6302.5 spectral lines set the value as 6173 and 6302, respectively.

Table B.1: Spin input file

cycle-number	:	1
obs-profiles(sav-file)	:	~/rahul/iqv_AR12353.sav
weight-Stokes <i>I</i>	:	1
weight-Stokes <i>Q</i>	:	2
weight-Stokes <i>U</i>	:	2
weight-Stokes <i>V</i>	:	5
wavelength	:	6173
Landé g-factor	:	2.5
iterations	:	100
invert	:	IQUV
line-centre	:	10
wave-sampling(Å)	:	0.02
heliocentric-angle (μ)	:	1
plot-profiles	:	1
normalized	:	1
instrumental_profile	:	profile.txt
initial-guess	:	1
S/N ratio	:	1000
xaxis	:	0,599
yaxis1	:	0,199
yaxis2	:	200,399
yaxis3	:	400,599
yaxis4	:	400,599
output(idl-sav)	:	~/rahul/inverted/

- **Landé g-factor:** The effective Landé g-factor of the spectral line used in the inversion.
- **iterations:** The maximum number of iteration performed for each pixels.
- **invert:** Set ‘IQUV’ and ‘IV’ to invert all four Stokes profiles, and Stokes *I* and *V* profiles, respectively.
- **line-centre:** The pixel value of the line center (rest wavelength position).
- **wave-sampling (Å):** It refers to the spectral sampling of the observed Stokes profiles.

- **heliocentric angle:** This value refers to the cosine of the heliocentric angle (θ), generally expressed as μ ($\cos \theta$). The default value is unity.
- **plot-profiles:** Set 1 to see the fitted and observed Stokes profiles.
- **normalized:** Set 1 if all observed Stokes profiles are normalized to quiet-sun intensity.
- **instrumental profile:** A file containing the instrumental profile data.
- **initial-guess:** Initial guess parameters will be evaluated if set to unity. Otherwise fixed guess model will be utilized.
- **S/N ratio:** The uncertainties in the observed Stokes profiles.
- **xaxis:** The pixels in the horizontal direction to be used in the inversion process.
- **yaxis[1,2,3,4]:** The pixels in the vertical direction to be used in the inversion process.
- **output (idl-sav):** The inverted output is stored in a standard IDL savefile.

B.3 Output files

SPIN writes the synthetic Stokes profiles and retrieve model parameters (such as magnetic field strength, LOS velocity, inclination and azimuthal angle *etc.*) in a standard IDL savefile. The model parameters and their errors are saved in a structure variable named as ‘inv’ whereas the synthetic Stokes profiles are saved in 4D float array, i.e. [xpixels, ypixels, λ , [I,Q,U,V]]. The *combine.pro* subroutine combines all the inverted regions. The *view_profiles.pro* can be used to display interactively the observed and best fitted Stokes profiles. The synthetic Stokes profiles can be viewed through a user-friendly IDL widget as shown in Figure B.1 (top panel), where the model parameters can be easily modified using the movable sliders. In addition to this, an IDL widget to carry out the inversion of the Stokes profiles is also developed (see bottom panel of B.1).

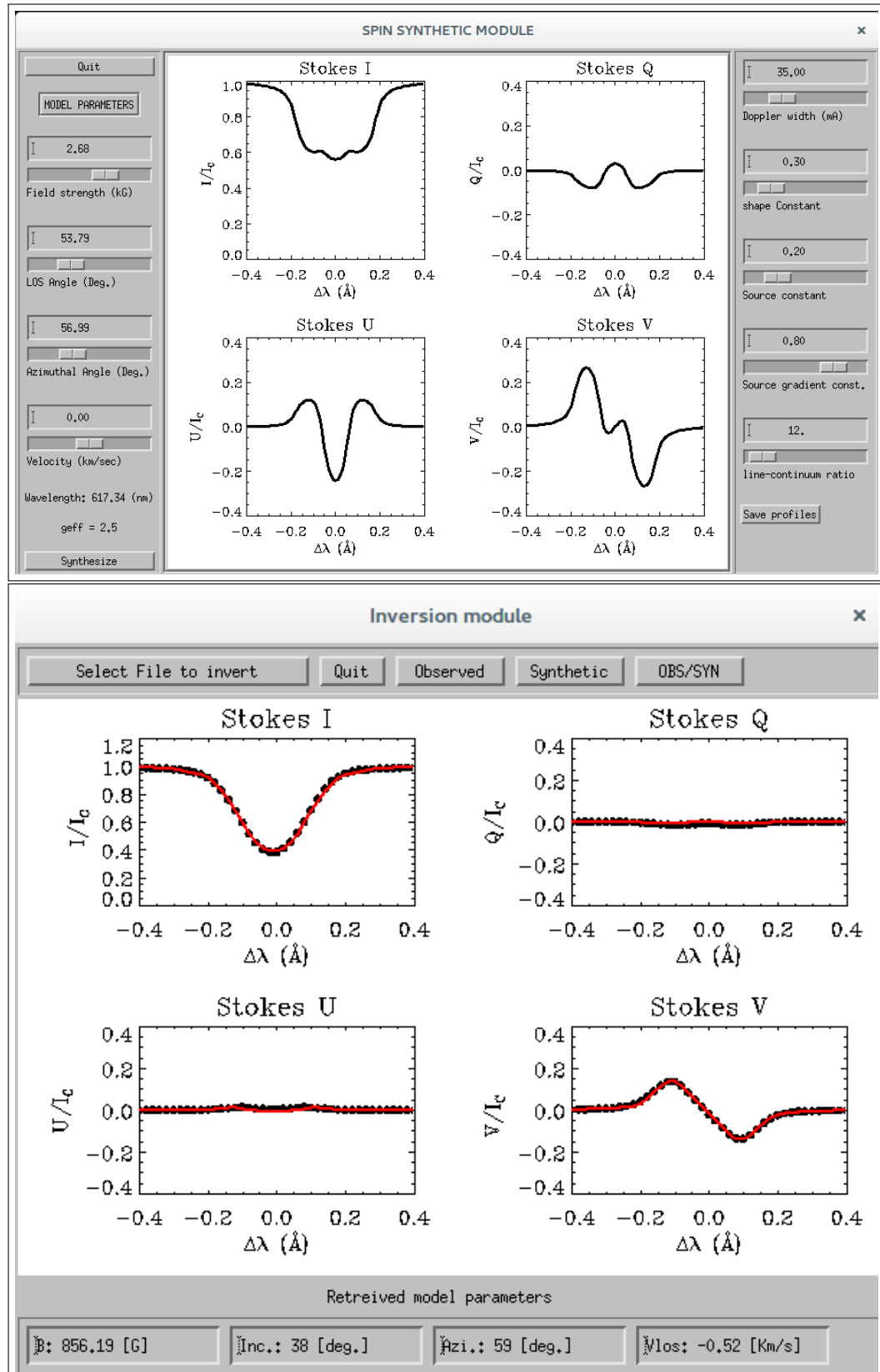


Figure B.1: *Top panel:* a snapshot of IDL widget showing the synthetic module. *Bottom panel:* a snapshot of inversion module. As an example, the filled black circles and solid red line represent the observed and best fitted profile, respectively.

Appendix C

C.1 Inversion of *Hinode*/SP data using SPIN

This appendix shows the inversion results of spectro-polarimetric data observed from *Hinode*/SP using SPIN code. To exhibit the performance of SPIN, the inverted maps of two active regions (NOAA AR 11899 and 11944) are demonstrated. The spectro-polarimetric data of AR 11899, which was located at $\mu = 0.98$, recorded from 0.5:00 to 05:24 UT on 20th November 2013, whereas AR 11944 ($\mu = 0.98$) recorded from 02:50 to 03:45 UT on 7th January 2014. Inversion scheme was same as described in Section 3.8.2, which was carried out across the 6302.5 Å spectral line for 41 wavelength points. The inverted maps of physical parameters such as magnetic field strength, inclination angle, azimuthal angle and LOS velocity obtained after the inversion of NOAA AR 11899 and 11944 are shown in Figure C.1 (AR 11899) and C.2 (AR 11944), respectively.

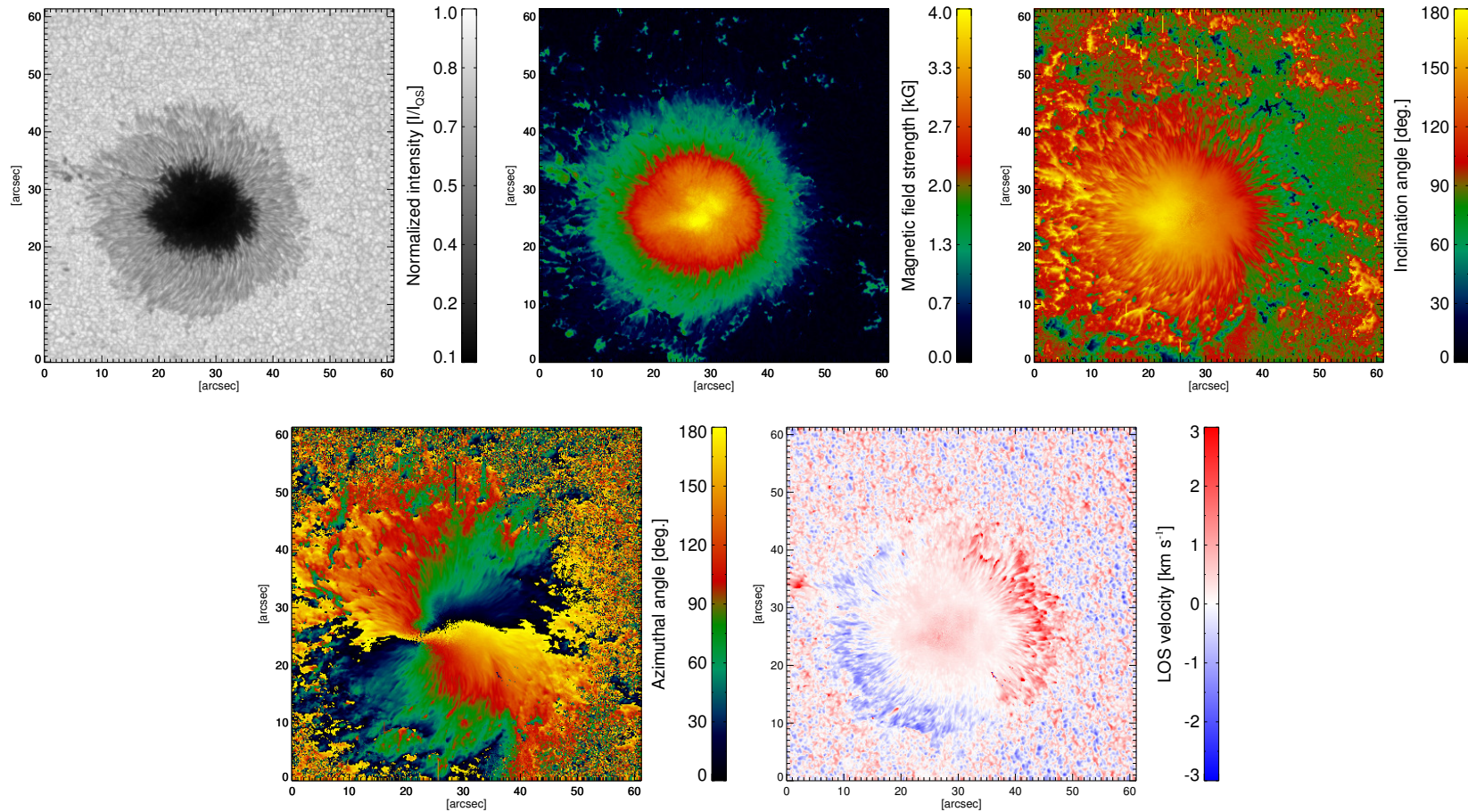


Figure C.1: Inverted parameters retrieved after the inversion of AR 11899 (observed by *Hinode*/SP) using SPIN code. *Top to bottom clockwise*: the normalized intensity map, magnetic field strength map, inclination angle map, azimuth angle map, and LOS velocity map.

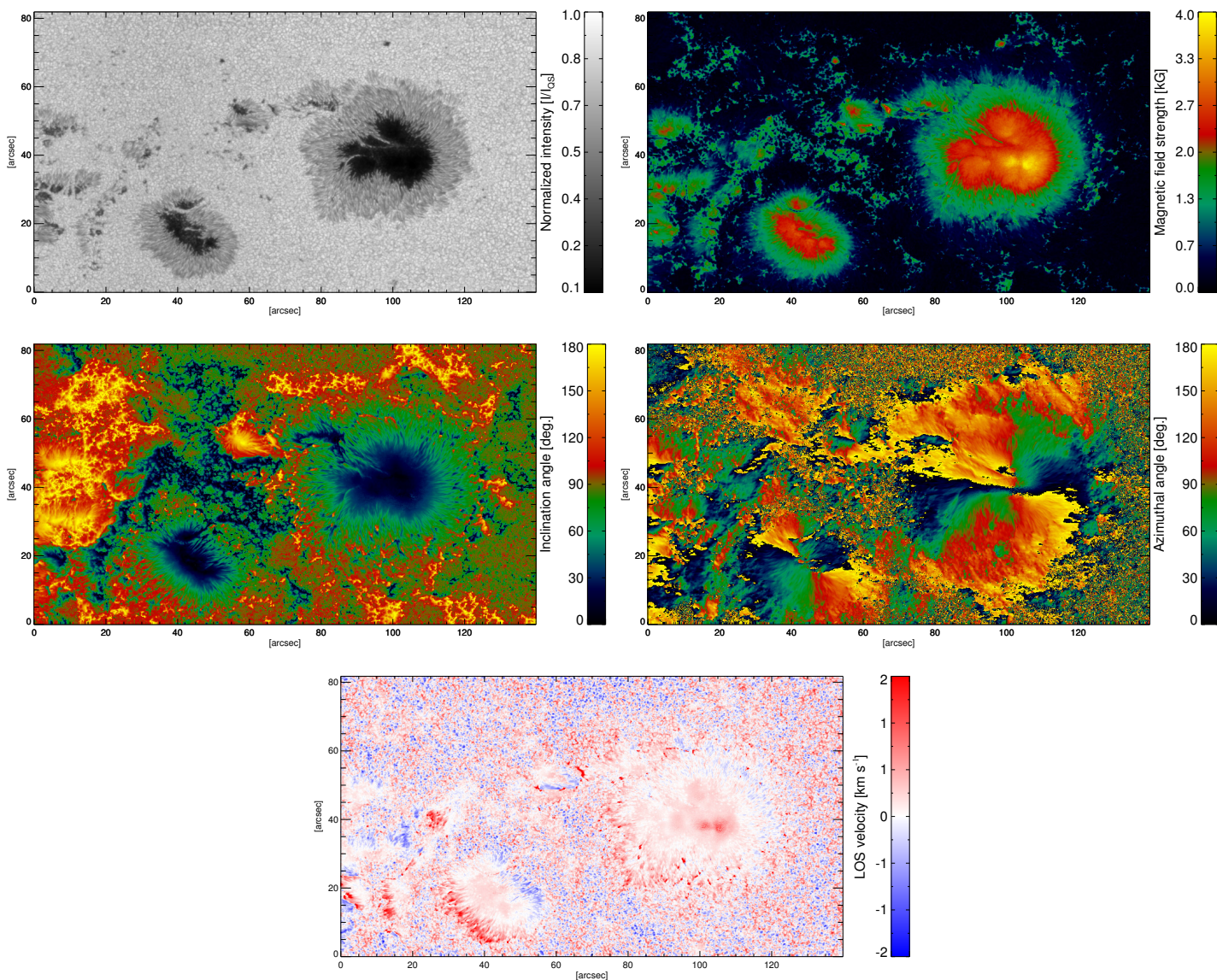


Figure C.2: Same as Figure C.1 but for AR 11944.

Bibliography

- Aschwanden, M. J.: 2005, *Physics of the Solar Corona. An Introduction with Problems and Solutions (2nd edition)*
- Asensio Ramos, A., Trujillo Bueno, J., and Landi Degl'Innocenti, E.: 2008, *Astrophys. J.* **683**, 542
- Auer, L. H., House, L. L., and Heasley, J. N.: 1977, *Solar Phys.* **55**, 47
- Barklem, P. S., Piskunov, N., and O'Mara, B. J.: 2000, *Astron. Astrophys. Suppl.* **142**, 467
- Baur, T. G., Elmore, D. E., Lee, R. H., Querfeld, C. W., and Rogers, S. R.: 1981, *Solar Phys.* **70**, 395
- Bellot Rubio, L. R.: 2006, in R. Casini and B. W. Lites (eds.), *Astron. Soc. Pac. Conf. Ser.*, Vol. 358 of *Astron. Soc. Pac. Conf. Ser.*, p. 107
- Bellot Rubio, L. R., Ruiz Cobo, B., and Collados, M.: 1998, *Astrophys. J.* **506**, 805
- Bharti, L., Beeck, B., and Schüssler, M.: 2010, *Astron. Astrophys.* **510**, A12
- Bharti, L., Joshi, C., and Jaaffrey, S. N. A.: 2007, *Astrophys. J.* **669**, L57
- Blackwell, D. E., Lynas-Gray, A. E., and Smith, G.: 1995, *Astron. Astrophys.* **296**, 217
- Born, M. and Wolf, E.: 1999, *Principles of optics : electromagnetic theory of propagation, interference and diffraction of light*
- Borrero, J. M. and Ichimoto, K.: 2011, *Liv. Rev. Solar Phys.* **8**, 4
- Borrero, J. M., Lagg, A., Solanki, S. K., and Collados, M.: 2005, *Astron. Astrophys.* **436**, 333
- Borrero, J. M., Lites, B. W., Lagg, A., Rezaei, R., and Rempel, M.: 2014, *Astron. Astrophys.* **572**, A54
- Borrero, J. M., Tomczyk, S., Kubo, M., Socas-Navarro, H., Schou, J., Couvidat, S., and Bogart, R.: 2011, *Solar Phys.* **273**, 267
- Bovelet, B. and Wiehr, E.: 2001, *Solar Phys.* **201**, 13
- Bray, R. J. and Loughhead, R. E.: 1964, *Sunspots*
- Bumba, V. and Suda, J.: 1983, *Bulletin of the Astronomical Institutes of Czechoslovakia* **34**, 29

- Cabrera Solana, D., Bellot Rubio, L. R., and del Toro Iniesta, J. C.: 2005, *Astron. Astrophys.* **439**, 687
- Carrington, R. C.: 1863, *Mon. Not. Roy. Astron. Soc.* **23**, 203
- Centeno, R., Schou, J., Hayashi, K., Norton, A., Hoeksema, J. T., Liu, Y., Leka, K. D., and Barnes, G.: 2014, *Solar Phys.* **289**, 3531
- Chandrasekhar, S.: 1960, *Radiative transfer*
- Chapman, G. A., Dobias, J. J., Preminger, D. G., and Walton, S. R.: 2003, *Geophysical Research Letters* **30(4)**, n/a, 1178
- Charbonneau, P.: 2010, *Liv. Rev. Solar Phys.* **7**, 3
- Cheung, M. C. M., Rempel, M., Title, A. M., and Schüssler, M.: 2010, *Astrophys. J.* **720**, 233
- Chevalier, S.: 1916, *Annales de l'Observatoire astronomique de Zô-sè (Chine), Tome IX, Page B1 - B16* 9
- Choudhuri, A. R.: 1986, *Astrophys. J.* **302**, 809
- Christensen-Dalsgaard, J., Gough, D. O., and Thompson, M. J.: 1991, *Astrophys. J.* **378**, 413
- Clark, D. H. and Stephenson, F. R.: 1978, *19*, 387
- Danielson, R. E.: 1961, *Astrophys. J.* **134**, 275
- de la Cruz Rodríguez, J. and van Noort, M.: 2016, *Space Sci. Rev.*
- del Toro Iniesta, J. C.: 2003, *Introduction to Spectropolarimetry*
- del Toro Iniesta, J. C. and Ruiz Cobo, B.: 2016, *Liv. Rev. Solar Phys.* **13(1)**, 4
- del Toro Iniesta, J. C., Tarbell, T. D., and Ruiz Cobo, B.: 1994, *Astrophys. J.* **436**, 400
- Denis, S., Coucke, P., Gabriel, E., Delrez, C., and Venkatakrishnan, P.: 2008, in *Ground-based and Airborne Telescopes II*, Vol. 7012 of *Proc. SPIE*, p. 701235
- Denis, S., Coucke, P., Gabriel, E., Delrez, C., and Venkatakrishnan, P.: 2010, in *Ground-based and Airborne Telescopes III*, Vol. 7733 of *Proc. SPIE*, p. 773335
- Denker, C., Tritschler, A., Deng, N., and Verdoni, A. P.: 2008, *Astronomische Nachrichten* **329**, 773
- Evershed, J.: 1909, *Mon. Not. Roy. Astron. Soc.* **69**, 454
- Feautrier, P.: 1964, *Comptes Rendus Academie des Sciences (serie non specifiee)* 258
- Fontenla, J. M., Avrett, E. H., and Loeser, R.: 1990, *Astrophys. J.* **355**, 700
- Frutiger, C.: 2000, *ETH, Zürich* p. No. 13896
- Frutiger, C., Solanki, S. K., Fligge, M., and Bruls, J. H. M. J.: 1999, in K. N. Nagendra and J. O. Stenflo (eds.), *Polarization*, Vol. 243 of *Astrophysics and Space Science Library*, pp 281–290

- Gabriel, A. H.: 1976, *Philosophical Transactions of the Royal Society of London Series A* **281**, 339
- Garcia de La Rosa, J. I.: 1987, *Solar Phys.* **112**, 49
- Gary, G. A.: 2001, *Solar Phys.* **203**, 71
- Gaunt, C. T.: 2016, *Space Weather* **14**(1), 2, 2015SW001306
- Gingerich, O., Noyes, R. W., Kalkofen, W., and Cuny, Y.: 1971, *Solar Physics* **18**(3), 347
- Goel, S. and Mathew, S. K.: 2014, *Solar Phys.* **289**, 1413
- Hale, G. E.: 1908, *Astrophys. J.* **28**, 315
- Hale, G. E.: 1924, *Nature* **113**, 105
- Hamedivafa, H.: 2011, *Solar Phys.* **270**, 75
- Hathaway, D. H.: 2015, *Liv. Rev. Solar Phys.* **12**, 4
- Hirzberger, J., Bonet, J. A., Sobotka, M., Vázquez, M., and Hanslmeier, A.: 2002, *Astron. Astrophys.* **383**, 275
- Hui, A., Armstrong, B., and Wray, A.: 1978, *Journal of Quantitative Spectroscopy and Radiative Transfer* **19**(5), 509
- Ichimoto, K., Lites, B., Elmore, D., Suematsu, Y., Tsuneta, S., Katsukawa, Y., Shimizu, T., Shine, R., Tarbell, T., Title, A., Kiyohara, J., Shinoda, K., Card, G., Lecinski, A., Streander, K., Nakagiri, M., Miyashita, M., Noguchi, M., Hoffmann, C., and Cruz, T.: 2008, *Solar Phys.* **249**, 233
- Ji, K., Jiang, X., Feng, S., Yang, Y., Deng, H., and Wang, F.: 2016, *Solar Phys.* **291**, 357
- Judge, P.: 2006, in J. Leibacher, R. F. Stein, and H. Uitenbroek (eds.), *Solar MHD Theory and Observations: A High Spatial Resolution Perspective*, Vol. 354 of *Astron. Soc. Pac. Conf. Ser.*, p. 259
- Jurčák, J., Martínez Pillet, V., and Sobotka, M.: 2006, *Astron. Astrophys.* **453**, 1079
- Katsukawa, Y., Yokoyama, T., Berger, T. E., Ichimoto, K., Kubo, M., Lites, B., Nagata, S., Shimizu, T., Shine, R. A., Suematsu, Y., Tarbell, T. D., Title, A. M., and Tsuneta, S.: 2007, *Pub. Astron. Soc. Japan* **59**, S577
- Keil, S. L., Rimmele, T., Keller, C. U., Hill, F., Radick, R. R., Oschmann, J. M., Warner, M., Dalrymple, N. E., Briggs, J., Hegwer, S. L., and Ren, D.: 2003, in S. L. Keil and S. V. Avakyan (eds.), *Innovative Telescopes and Instrumentation for Solar Astrophysics*, Vol. 4853 of *Proc. SPIE*, pp 240–251
- Kilcik, A., Yurchyshyn, V. B., Rempel, M., Abramenko, V., Kitai, R., Goode, P. R., Cao, W., and Watanabe, H.: 2012, *Astrophys. J.* **745**, 163
- Kitai, R., Watanabe, H., Nakamura, T., Otsuji, K.-I., Matsumoto, T., Ueno, S., Nagata, S., Shibata, K., Muller, R., Ichimoto, K., Tsuneta, S., Suematsu, Y., Katsukawa, Y., Shimizu, T., Tarbell, T. D., Shine, R. A., Title, A. M., and Lites, B.: 2007, *Pub. Astron. Soc. Japan* **59**, 585

- Kneer, F.: 1973, *Solar Phys.* **28**, 361
- Kopp, G. and Rabin, D.: 1992, *Solar Phys.* **141**, 253
- Kosugi, T., Matsuzaki, K., Sakao, T., Shimizu, T., Sone, Y., Tachikawa, S., Hashimoto, T., Minesugi, K., Ohnishi, A., Yamada, T., Tsuneta, S., Hara, H., Ichimoto, K., Suematsu, Y., Shimojo, M., Watanabe, T., Shimada, S., Davis, J. M., Hill, L. D., Owens, J. K., Title, A. M., Culhane, J. L., Harra, L. K., Doschek, G. A., and Golub, L.: 2007, *Solar Phys.* **243**, 3
- Lagg, A., Lites, B., Harvey, J., Gosain, S., and Centeno, R.: 2015, *Space Sci. Rev.*
- Lagg, A., Woch, J., Krupp, N., and Solanki, S. K.: 2004, *Astron. Astrophys.* **414**, 1109
- Landi Degl'Innocenti, E. and Landi Degl'Innocenti, M.: 1985, *Solar Phys.* **97**, 239
- Landi Degl'Innocenti, E. and Landolfi, M.: 1982, *Solar Phys.* **77**, 13
- Landi Degl'Innocenti, E. and Landolfi, M. (eds.): 2004, *Polarization in Spectral Lines*, Vol. 307 of *Astrophysics and Space Science Library*
- Leka, K. D.: 1997, *Astrophys. J.* **484**, 900
- Leka, K. D., Barnes, G., and Crouch, A.: 2009, in B. Lites, M. Cheung, T. Magara, J. Mariska, and K. Reeves (eds.), *The Second Hinode Science Meeting: Beyond Discovery-Toward Understanding*, Vol. 415 of *Astron. Soc. Pac. Conf. Ser.*, p. 365
- Lites, B., Casini, R., Garcia, J., and Socas-Navarro, H.: 2007, *Mem. Soc. Astron. Ital.* **78**, 148
- Lites, B. W.: 1987, *ApOpt* **26**, 3838
- Lites, B. W., Scharmer, G. B., Berger, T. E., and Title, A. M.: 2004, *Solar Phys.* **221**, 65
- Livingston, W.: 2002, *Solar Phys.* **207**, 41
- López Ariste, A. and Semel, M.: 1999, *Astron. Astrophys.* **350**, 1089
- Louis, R. E.: 2016, *Astronomische Nachrichten* **337**, 1033
- Louis, R. E., Bayanna, A. R., Mathew, S. K., and Venkatakrishnan, P.: 2008, *Solar Phys.* **252**, 43
- Louis, R. E., Bellot Rubio, L. R., de la Cruz Rodríguez, J., Socas-Navarro, H., and Ortiz, A.: 2015, *Astron. Astrophys.* **584**, A1
- Louis, R. E., Bellot Rubio, L. R., Mathew, S. K., and Venkatakrishnan, P.: 2009, *Astrophys. J.* **704**, L29
- Louis, R. E., Mathew, S. K., Bellot Rubio, L. R., Ichimoto, K., Ravindra, B., and Raja Bayanna, A.: 2012a, *Astrophys. J.* **752**, 109
- Louis, R. E., Ravindra, B., Mathew, S. K., Bellot Rubio, L. R., Raja Bayanna, A., and Venkatakrishnan, P.: 2012b, *Astrophys. J.* **755**, 16

- Lucy, L. B.: 1974, *Astronom. J.* **79**, 745
- Maltby, P.: 1977, *Solar Phys.* **55**, 335
- Maltby, P., Avrett, E. H., Carlsson, M., Kjeldseth-Moe, O., Kurucz, R. L., and Loeser, R.: 1986, *Astrophys. J.* **306**, 284
- Mathew, S. K.: 2009, in S. V. Berdyugina, K. N. Nagendra, and R. Ramelli (eds.), *Solar Polarization 5: In Honor of Jan Stenflo*, Vol. 405 of *Astron. Soc. Pac. Conf. Ser.*, p. 461
- Mathew, S. K., Bayanna, A. R., Tiwary, A. R., Bireddy, R., and Venkatakrishnan, P.: 2017, *Solar Physics* **292**(8), 106
- Mathew, S. K., Lagg, A., Solanki, S. K., Collados, M., Borrero, J. M., Berdyugina, S., Krupp, N., Woch, J., and Frutiger, C.: 2003, *Astron. Astrophys.* **410**, 695
- Mathew, S. K., Martínez Pillet, V., Solanki, S. K., and Krivova, N. A.: 2007, *Astron. Astrophys.* **465**, 291
- Mathew, S. K., Solanki, S. K., Lagg, A., Collados, M., Borrero, J. M., and Berdyugina, S.: 2004, *Astron. Astrophys.* **422**, 693
- Mathew, S. K., Zakharov, V., and Solanki, S. K.: 2009, *Astron. Astrophys.* **501**, L19
- Maurya, R. A. and Ambastha, A.: 2010, *Astrophys. J.* **714**, L196
- McIntosh, P. S.: 1990, *Solar Phys.* **125**, 251
- Metcalf, T. R.: 1994, *Solar Phys.* **155**, 235
- Mohanakrishna, R., Bayanna, A. R., Sankarasubramanian, K., and Mathew, S. K.: 2017, *in preparation*
- Montesinos, B. and Thomas, J. H.: 1997, *Nature* **390**, 485
- Muller, R.: 1973, *Solar Phys.* **29**, 55
- Muller, R.: 1976, *Solar Phys.* **48**, 101
- Muller, R.: 1979, *Solar Phys.* **61**, 297
- Nave, G., Johansson, S., Learner, R. C. M., Thorne, A. P., and Brault, J. W.: 1994, *Astrophys. J. Sup. Ser.* **94**, 221
- Orozco Suárez, D. and Del Toro Iniesta, J. C.: 2007, *Astron. Astrophys.* **462**, 1137
- Ortiz, A., Bellot Rubio, L. R., and Rouppe van der Voort, L.: 2010, *Astrophys. J.* **713**, 1282
- Parker, E. N.: 1979, *Astrophys. J.* **234**, 333
- Pesnell, W. D., Thompson, B. J., and Chamberlin, P. C.: 2012, *Solar Phys.* **275**, 3
- Pettauer, T. and Brandt, P. N.: 1997, *Solar Phys.* **175**, 197

- Pierce, A. K. and Slaughter, C. D.: 1977, *Solar Phys.* **51**, 25
- Press, W. H., Teukolsky, S. A., Vetterling, W. T., and Flannery, B. P.: 1992, *Numerical recipes in FORTRAN. The art of scientific computing*
- Pulkkinen, T.: 2007, *Liv. Rev. Solar Phys.* **4**, 1
- Rachkovsky, D. N.: 1962, *Izvestiya Ordona Trudovogo Krasnogo Znameni Krymskoy Astrofizicheskoy Observatorii* **28**, 259
- Rachkovsky, D. N.: 1967, *Izvestiya Ordona Trudovogo Krasnogo Znameni Krymskoy Astrofizicheskoy Observatorii* **37**, 56
- Raja Bayanna, A., Mathew, S. K., Venkatakrishnan, P., and Srivastava, N.: 2014, *Solar Phys.* **289**, 4007
- Raouafi, N. E., Riley, P., Gibson, S., Fineschi, S., and Solanki, S. K.: 2016, *Frontiers in Astronomy and Space Sciences* **3**, 20
- Rees, D. E., Durrant, C. J., and Murphy, G. A.: 1989, *Astrophys. J.* **339**, 1093
- Rempel, M. and Schlichenmaier, R.: 2011, *Liv. Rev. Solar Phys.* **8**, 3
- Rempel, M., Schüssler, M., and Knölker, M.: 2009, *Astrophys. J.* **691**, 640
- Richardson, W. H.: 1972, *Journal of the Optical Society of America (1917-1983)* **62**, 55
- Riethmüller, T. L., Solanki, S. K., van Noort, M., and Tiwari, S. K.: 2013, *Astron. Astrophys.* **554**, A53
- Riethmüller, T. L., Solanki, S. K., Zakharov, V., and Gandorfer, A.: 2008, *Astron. Astrophys.* **492**, 233
- Rimmele, T.: 2008, *Astrophys. J.* **672**, 684
- Rimmele, T. R.: 1997, *Astrophys. J.* **490**, 458
- Ruiz Cobo, B. and del Toro Iniesta, J. C.: 1992, *Astrophys. J.* **398**, 375
- Scharmer, G. B., Nordlund, Å., and Heinemann, T.: 2008, *Astrophys. J.* **677**, L149
- Scherrer, P. H., Bogart, R. S., Bush, R. I., Hoeksema, J. T., Kosovichev, A. G., Schou, J., Rosenberg, W., Springer, L., Tarbell, T. D., Title, A., Wolfson, C. J., Zayer, I., and MDI Engineering Team: 1995, *Solar Phys.* **162**, 129
- Scherrer, P. H., Schou, J., Bush, R. I., Kosovichev, A. G., Bogart, R. S., Hoeksema, J. T., Liu, Y., Duvall, T. L., Zhao, J., Title, A. M., Schrijver, C. J., Tarbell, T. D., and Tomczyk, S.: 2012, *Solar Phys.* **275**, 207
- Schlichenmaier, R. and Collados, M.: 2002, *Astron. Astrophys.* **381**, 668
- Schlichenmaier, R., Jahn, K., and Schmidt, H. U.: 1998, *Astron. Astrophys.* **337**, 897
- Schlichenmaier, R., Rezaei, R., Bello González, N., and Waldmann, T. A.: 2010, *Astron. Astrophys.* **512**, L1

- Schmidt, W., von der Lühe, O., Volkmer, R., Denker, C., Solanki, S. K., Balthasar, H., Bello Gonzalez, N., Berkefeld, T., Collados, M., Fischer, A., Halbgewachs, C., Heidecke, F., Hofmann, A., Kneer, F., Lagg, A., Nicklas, H., Popow, E., Puschmann, K. G., Schmidt, D., Sigwarth, M., Sobotka, M., Soltau, D., Staude, J., Strassmeier, K. G., and Waldmann , T. A.: 2012, *Astronomische Nachrichten* **333**, 796
- Schrijver, C. J.: 2015, *Space Weather* **13(9)**, 524, 2015SW001252
- Schüssler, M. and Rempel, M.: 2005, *Astron. Astrophys.* **441**, 337
- Schüssler, M. and Vögler, A.: 2006, *Astrophys. J.* **641**, L73
- Schwabe, H.: 1844, *Astronomische Nachrichten* **21(15)**, 234
- Skumanich, A. and Lites, B. W.: 1987, *Astrophys. J.* **322**, 473
- Sobotka, M.: 1997, in B. Schmieder, J. C. del Toro Iniesta, and M. Vazquez (eds.), *1st Advances in Solar Physics Euroconference. Advances in Physics of Sunspots*, Vol. 118 of *Astronomical Society of the Pacific Conference Series*, p. 155
- Sobotka, M., Bonet, J. A., and Vazquez, M.: 1993, *Astrophys. J.* **415**, 832
- Sobotka, M., Bonet, J. A., and Vazquez, M.: 1994, *Astrophys. J.* **426**, 404
- Sobotka, M., Brandt, P. N., and Simon, G. W.: 1997, *Astron. Astrophys.* **328**, 682
- Sobotka, M., Brandt, P. N., and Simon, G. W.: 1999a, *Astron. Astrophys.* **348**, 621
- Sobotka, M. and Hanslmeier, A.: 2005, *Astron. Astrophys.* **442**, 323
- Sobotka, M. and Puschmann, K. G.: 2009, *Astron. Astrophys.* **504**, 575
- Sobotka, M., Vázquez, M., Bonet, J. A., Hanslmeier, A., and Hirzberger, J.: 1999b, *Astrophys. J.* **511**, 436
- Socas-Navarro, H.: 2001, in M. Sigwarth (ed.), *Advanced Solar Polarimetry – Theory, Observation, and Instrumentation*, Vol. 236 of *Astronomical Society of the Pacific Conference Series*, p. 487
- Socas-Navarro, H.: 2015, *NICOLE: NLTE Stokes Synthesis/Inversion Code*, Astrophysics Source Code Library
- Socas-Navarro, H., Martínez Pillet, V., Sobotka, M., and Vázquez, M.: 2004, *Astrophys. J.* **614**, 448
- Solanki, S. K.: 1986, *Astron. Astrophys.* **168**, 311
- Solanki, S. K.: 1993, *Space Sci. Rev.* **63**, 1
- Solanki, S. K.: 2003, *Astron. Astrophys. Rev.* **11**, 153
- Solanki, S. K. and Montavon, C. A. P.: 1993, *Astron. Astrophys.* **275**, 283
- Solanki, S. K., Schüssler, M., and Fligge, M.: 2000, *Nature* **408**, 445

- Solanki, S. K., Schüssler, M., and Fligge, M.: 2002, *Astron. Astrophys.* **383**, 706
- Song, D., Chae, J., Yurchyshyn, V., Lim, E.-K., Cho, K.-S., Yang, H., Cho, K., and Kwak, H.: 2017, *Astrophys. J.* **835**, 240
- Spruit, H. C. and Scharmer, G. B.: 2006, *Astron. Astrophys.* **447**, 343
- Stenflo, J. (ed.): 1994, *Solar Magnetic Fields: Polarized Radiation Diagnostics*, Vol. 189 of *Astrophysics and Space Science Library*
- Stenflo, J. O.: 2015, *Space Sci. Rev.*
- Stix, M.: 2004, *The sun : an introduction*
- Suematsu, Y., Tsuneta, S., Ichimoto, K., Shimizu, T., Otsubo, M., Katsukawa, Y., Nakagiri, M., Noguchi, M., Tamura, T., Kato, Y., Hara, H., Kubo, M., Mikami, I., Saito, H., Matsushita, T., Kawaguchi, N., Nakaoji, T., Nagae, K., Shimada, S., Takeyama, N., and Yamamuro, T.: 2008, *Solar Phys.* **249**, 197
- Thomas, J. H. and Weiss, N. O. (eds.): 1992, *Sunspots: Theory and observations; Proceedings of the NATO Advanced Research Workshop on the Theory of Sunspots, Cambridge, United Kingdom, Sept. 22-27, 1991*, Vol. 375 of *NATO Advanced Science Institutes (ASI) Series C*
- Thomas, J. H., Weiss, N. O., Tobias, S. M., and Brummell, N. H.: 2002, *Nature* **420**, 390
- Tiwary, A. R., Mathew, S. K., Bayanna, A. R., Venkatakrishnan, P., and Yadav, R.: 2017, *Solar Physics* **292**(4), 49
- Tritschler, A. and Schmidt, W.: 2002, *Astron. Astrophys.* **388**, 1048
- Trujillo Bueno, J.: 2001, in M. Sigwarth (ed.), *Advanced Solar Polarimetry – Theory, Observation, and Instrumentation*, Vol. 236 of *Astronomical Society of the Pacific Conference Series*, p. 161
- Tsuneta, S., Ichimoto, K., Katsukawa, Y., Nagata, S., Otsubo, M., Shimizu, T., Suematsu, Y., Nakagiri, M., Noguchi, M., Tarbell, T., Title, A., Shine, R., Rosenberg, W., Hoffmann, C., Jurcevich, B., Kushner, G., Levay, M., Lites, B., Elmore, D., Matsushita, T., Kawaguchi, N., Saito, H., Mikami, I., Hill, L. D., and Owens, J. K.: 2008, *Solar Phys.* **249**, 167
- Unno, W.: 1956, *Pub. Astron. Soc. Japan* **8**, 108
- Švanda, M., Klvaňa, M., and Sobotka, M.: 2009, *Astron. Astrophys.* **506**, 875
- Venkatakrishnan, P., Mathew, S. K., Srivastava, N., Bayanna, A. R., Kumar, B., Ramya, B., Naresh, J., and Saradava, M.: 2017, *Current Science* 113, No. 4
- Vernazza, J. E., Avrett, E. H., and Loeser, R.: 1981, *Astrophys. J. Sup. Ser.* **45**, 635
- Watanabe, H.: 2014, *Pub. Astron. Soc. Japan* **66**, S1
- Watanabe, H., Bellot Rubio, L. R., de la Cruz Rodríguez, J., and Rouppe van der Voort, L.: 2012, *Astrophys. J.* **757**, 49

- Watanabe, H., Kitai, R., and Ichimoto, K.: 2009, *Astrophys. J.* **702**, 1048
- Weiss, N. O.: 2002, *Astronomische Nachrichten* **323**, 371
- Westendorp Plaza, C., del Toro Iniesta, J. C., Ruiz Cobo, B., Martinez Pillet, V., Lites, B. W., and Skumanich, A.: 1997, *Nature* **389**, 47
- Westendorp Plaza, C., del Toro Iniesta, J. C., Ruiz Cobo, B., Martínez Pillet, V., Lites, B. W., and Skumanich, A.: 1998, *Astrophys. J.* **494**, 453
- Westendorp Plaza, C., del Toro Iniesta, J. C., Ruiz Cobo, B., Martínez Pillet, V., Lites, B. W., and Skumanich, A.: 2001, *Astrophys. J.* **547**, 1130
- Wittmann, A.: 1974, *Solar Phys.* **35**, 11
- Wittmann, A. D. and Xu, Z. T.: 1987, *Astron. Astrophys. Suppl.* **70**, 83
- Yadav, R., Louis, R. E., and Mathew, S. K.: 2017a, *submitted to Astrophys. J.*
- Yadav, R. and Mathew, S. K.: 2017, *submitted to Solar Physics*
- Yadav, R., Mathew, S. K., and Tiwary, A. R.: 2017b, *Solar Physics* **292(8)**, 105
- Yariv, A., *Optical electronics*, Holt McDougal, Third Ed
- Zeeman, P.: 1897, *Nature* **55**, 347
- Zhang, Y. and Ichimoto, K.: 2013, *Astron. Astrophys.* **560**, A77
- Zwaan, C.: 1978, *Solar Phys.* **60**, 213
- Zwaan, C.: 1985, *Solar Phys.* **100**, 397
- Zwaan, C.: 1987, *Ann. Rev. Astron. Astrophys.* **25**, 83

Publications attached with the thesis

1. “*SPIN: An Inversion Code for the Photospheric Spectral Line*”
Rahul Yadav, Shibu K. Mathew and Alok Ranjan Tiwary, *Solar Phys.* (2017) 292:105.